

# Role of Interfacial Resistance to Shear Stress on Adhesive Peel Strength

Nicolas Amouroux,<sup>†</sup> Jérôme Petit, and Liliane Léger\*

Laboratoire de Physique de la Matière Condensée, Collège de France, Unité de Recherche Associée Centre National de la Recherche Scientifique 792, 11, pl. Marcelin Berthelot, 75231 Paris Cedex 05, France

Received January 29, 2001. In Final Form: July 5, 2001

The adherence of an acrylic tape on silicone elastomers containing various quantities of a silicone MQ resin has been investigated by an instrumented peel test, along the lines of Newby and Chaudhury's work (*Langmuir* **1997**, *13*, 1805–1809; *Langmuir* **1998**, *14*, 4865–4872), which gave the first evidence of interfacial slip when a pressure-sensitive adhesive is peeled from a thin poly(dimethylsiloxane) (PDMS) layer. In the present study, we show that the amplitude of interfacial slip movements is correlated to the composition of the elastomer in MQ resin (small silica-like particles inserted into the elastomer). High slip amplitudes are associated with low MQ resin content and result in weak shear deformations in the adhesive. Thus, depending on the composition of the elastomer, the peel energy is dominated either by frictional losses associated with slip at the interface (low MQ resin content) or by viscous dissipation due to shear deformations distributed in the volume of the adhesive (high MQ resin content). The transition between these two processes depends on the contact time between the acrylic tape and the elastomer prior to peeling. The viscous and the frictional parts of the dissipated energy are quantitatively estimated from the observed displacements at the interface and within the adhesive, the shear modulus of the adhesive, and frictional laws determined from "pure" shear experiments. The computed energies can represent half of the measured peel energy for this adjustable slip system. The understanding of the molecular mechanisms involved should help in the design of surfaces with adjusted adhesive properties.

## Introduction

It is now well-known that peeling viscoelastic materials involves several dissipative mechanisms, localized in different zones relative to the fracture tip. At the fracture tip, the adhesion energy  $W = \gamma_1 + \gamma_2 - \gamma_{12}$  (where  $\gamma_1$  and  $\gamma_2$  are the surface tension of the adhesive and of the substrate, respectively, and  $\gamma_{12}$  is the interfacial tension between the adhesive and the substrate) is necessary to separate the two bodies and create new free surfaces (Dupré). In the case of viscoelastic materials, the triple line (substrate–adhesive–air contact line) is not straight but forms a periodic pattern due to instability analogous to the meniscus instability in hydrodynamics. For the system investigated here, the typical wavelength is in the 100  $\mu\text{m}$  range. This periodic structure leads to the formation of columns of adhesive that are elongated in the direction of the peel force. The corresponding work of elongation may represent an important part of the peel energy.<sup>1–3</sup> Some work can also be dissipated far from the fracture tip in a zone where the curvature of the adhesive tape is large. This mechanism was analyzed by Loukis and Aravas.<sup>4</sup> The curvature of the tape induces a compression zone, which was modeled and evidenced by Kaelble.<sup>5,6</sup> This compression gives birth to a shear stress field. The details of the processes occurring in this zone are precisely the object of the present paper.

The resistance of the interface to shear stress could indeed have an important effect on the final peel force. Peeling a viscoelastic tape or a silicone elastomer<sup>7,8</sup> from a glass grafted with poly(dimethylsiloxane) (PDMS) chains, Newby and Chaudhury clearly evidenced slip motions of the adhesive on the substrate, using tracking fluorescent particles placed at the interface. This reveals a very small resistance of this interface to shear stress. Surprisingly enough, they detected no significant slip movements when the same adhesive was peeled from a perfluorinated glass. The low peel force on PDMS could then be explained by a propagation of the fracture through interfacial slip, which allows the shear stress to relax in the adhesive. On perfluorinated glass, no significant slip was detected and the peel force was higher than for the PDMS/adhesive system, even if the corresponding work of adhesion was smaller.

Following these ideas, we designed systematic experiments aimed at better understanding the role of interfacial resistance on shear stress in peel experiments, using as substrates series of silicone elastomers made of poly(dimethylsiloxane) chains co-cross-linked with a silicone MQ resin. The proportion of MQ resin in the elastomer is known to adjust (enhance) the peel force versus a given adhesive.

The paper is organized as follows: the descriptions of the technique, the substrate preparation, and adhesives used are gathered in the Experimental Section. In the Results Section, the mechanical characteristics of the elastomers used, the typical peel force versus peel velocity curves, and the experimental determination of the displacements both at the adhesive–elastomer interface and in the middle of the adhesive layer are reported. Finally,

\* To whom correspondence should be addressed: e-mail liliane.leger@college-de-france.fr.

<sup>†</sup> Present address: Laboratoire d'Etude des Matériaux, ELF Atochem, CERDATO, 27470, Serquigny, France. E-mail nicolas.amouroux@atofina.com.

(1) Good, J.; Gupta, R. K. *J. Adhes.* **1998**, *26*, 13–136.

(2) Benyahia, L.; Verdier, C.; Piau, J. M. *J. Adhes.* **1997**, *61*, 45–73.

(3) Derail, C.; Allal, A.; Marin, G.; Tordjeman, P. *J. Adhes.* **1997**, *61*, 123–157.

(4) Loukis, M. J.; Aravas, N. *J. Adhes.* **1991**, *35*, 7–22.

(5) Kaelble, D. H. *Trans. Soc. Rheol.* **1960**, *4*, 45–73.

(6) Kaelble, D. H. *Trans. Soc. Rheol.* **1974**, *18* (2), 219–235.

(7) Newby, B. M.; Chaudhury, M. K. *Langmuir* **1997**, *13*, 1805–1809.

(8) Newby, B. M.; Chaudhury, M. K. *Langmuir* **1998**, *14*, 4865–4872.

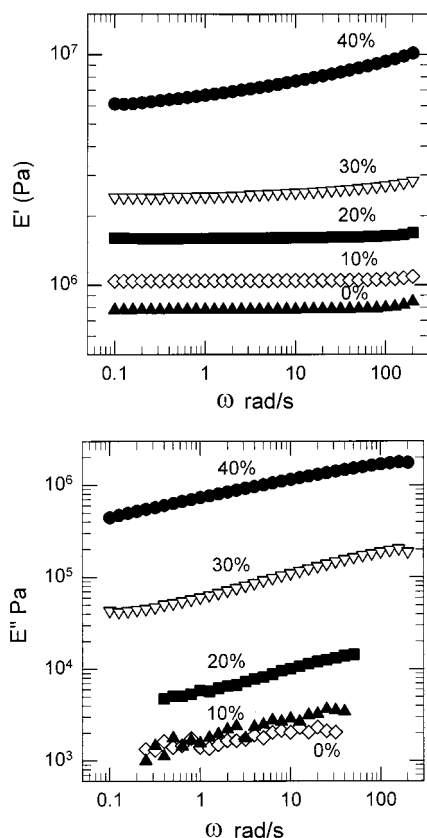


**Figure 1.** Elastic,  $E'$ , and loss,  $E''$ , components of the complex Young modulus at room temperature (25 °C) versus the pulsation  $\omega$  for elastomers containing between 0% and 40% silicone MQ resin.

these results are discussed: the consequences of either interfacial slip or shear deformations in the adhesive layer on the value of the peel energy are estimated and compared.

## Results

**Material Properties.** The storage and loss moduli of the different elastomers used are reported in Figure 1. The storage moduli,  $E'$ , increase from  $8 \times 10^5$  Pa for pure PDMS elastomers up to  $6 \times 10^6$  Pa for an elastomer filled with 40% (by weight) in MQ resin. The loss moduli,  $E''$ , increase much more, gaining three orders of magnitude between small resin content ( $\sim 10^3$  Pa) and 40 wt % resin content ( $\sim 10^6$  Pa). The elastomers remain, however, essentially elastic since  $\tan \delta = E''/E'$  remains smaller than 0.1 in any case.

In contrast to bulk mechanical properties, the surface energies appear rather independent of the resin content. The dispersive component of surface energy is equal to  $\gamma^D = 21 \pm 1$  mN/m for all the samples, while the nondispersive component slightly increases from  $\gamma^{ND} \sim 0$  to  $2 \pm 1$  mN/m between 0% and 40% resin content.

In Figure 2, the master curves for the components of the complex shear moduli as a function of reduced frequency for the acrylic adhesive used (3M Scotch 600) are displayed. Compared to the silicone elastomers, the adhesive is much softer.

**Peel  $G$ - $V$  Curves.** Acrylic adhesive tapes were peeled from thin layers of silicone elastomers containing between 0 and 40 wt % MQ resin, supported on glass slides, and from pure resin layers deposited on glass. The resulting energy release rates,  $G$ , versus the peel velocity,  $V$ , are shown in Figure 3, for contact times between the adhesive

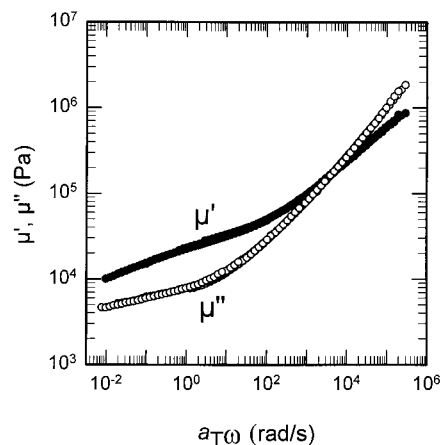


**Figure 2.** Elastic,  $\mu'$ , and loss,  $\mu''$ , components of the complex shear modulus at a reference temperature (25 °C) versus the reduced pulsation,  $a_T \omega$ , for the 3M 600 adhesive.

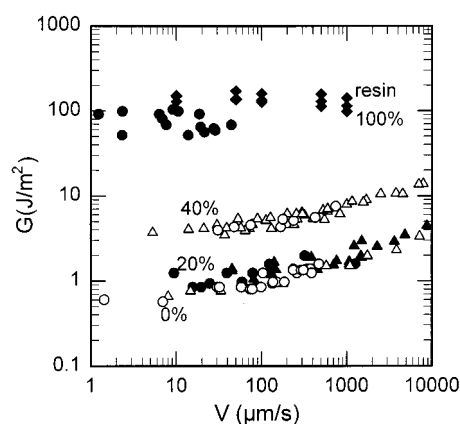


**Figure 3.** Energy release rate,  $G$ , versus peel velocity,  $V$ , for elastomer substrates containing 0%, 20%, and 40% MQ resin and for the pure resin substrate. Triangle symbols represent points obtained with simple adhesive tapes (17 μm thick), while circles are for doubled adhesive tapes (35 μm thick). Diamonds symbols refer to peel at imposed velocity (simple tape), whereas all the other points were obtained at constant load.

and the silicone layer prior to peeling between 5 and 8 days. The dependence on peel velocity is a slowly monotonically increasing function. In contrast, the  $G$  values increase roughly exponentially with the resin content, reaching very large values of the order of  $\sim 100$  J/m<sup>2</sup> on pure resin. The  $G$ - $V$  curves are not sensitive to the adhesive thickness: similar results were obtained for 17 μm and 35 μm thick adhesive layers.

**Displacements.** During the peel experiment, the displacements of small fluorescent latex particles (1 μm in diameter) placed either at the acrylic/silicone interface or in the middle of the adhesive film (doubled films) were monitored by use of an optical microscope coupled with a CCD camera, a videotape recorder, and an image software analysis. A typical video sequence and the corresponding trajectory of *one* probe particle are presented in Figure 4. When the peel front is still far, the particle remains immobile, and it starts to move parallel to the interfacial plane, in the same direction as the peel front, at a given distance from the peel front. The direction of motion is then reversed when the peel front is close enough to the particle. Finally the particle disappears from the field of view as it is taken away with the peeled ribbon. The trajectories of the probes look like damped sinusoidal functions. Displacements  $u$  (i.e., distance

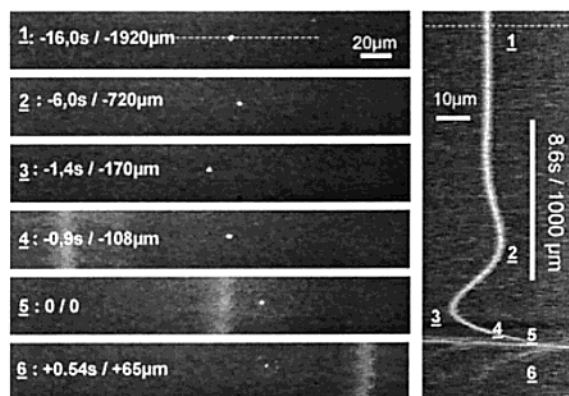


**Figure 4.** Typical video sequence showing the displacement of a latex particle placed at the interface between the adhesive and an elastomer substrate. The peel velocity is  $V = 120 \mu\text{m/s}$ . The first image shows the particle when the peel front is far. As the front approaches the particle first goes to the right ( $u_s > 0$ , image 2), then to the left, toward the front ( $u_s < 0$ , image 3), and eventually changes its direction again when the front is very close (images 4 and 5). After the delamination, the latex particle is still visible for a while before leaving the depth of field. On the right, the corresponding trajectory of the particle (position as a function of time) is presented. The peel front is visible as the vertical straight line in the three lower left pictures. The trajectory of the peel front appears as the inclined white straight line at the bottom of the right picture. The slope of this line is the peel velocity.

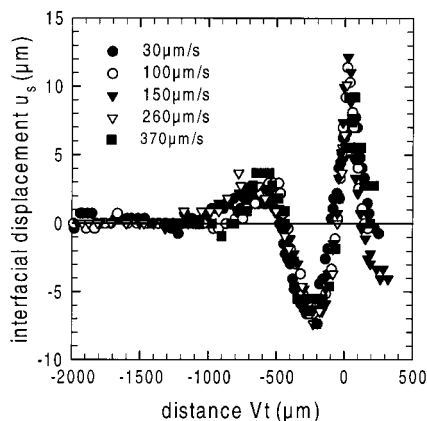


**Figure 5.** Displacements at the interface  $u_s$  for the 0% elastomer layer for different peel velocities after a long contact time prior to peel. All the trajectories collapse on a single master curve when plotted as a function of  $Vt$ .

between the actual position of the particle and the position it had far from the peel front) in a plane parallel to the interface are taken as positive when the probe goes in the same direction as the peel front. The uncertainty in the determination of the displacements is less than a micrometer (on the order of the size of the particle). The displacements  $u_s$  and  $u_v$  of the probes—where the subscript  $s$  stands for the probe placed initially at the surface of the adhesive (i.e., at the adhesive–elastomer interface) and  $v$  for probe in the volume (midlayer of the adhesive)—were found to be rather independent of the peel velocity in the range investigated (10–1000  $\mu\text{m/s}$ ) when plotted as a function of the distance between the peel front and the first (unperturbed) position of the probe,  $Vt$  (with  $V$  the peel front velocity and  $t$  the time). This remarkable property is illustrated in Figure 5 for a peel experiment on a pure PDMS elastomer layer. The displacements  $u_v$  and  $u_s$  are shown for elastomers containing 0%, 20%, and

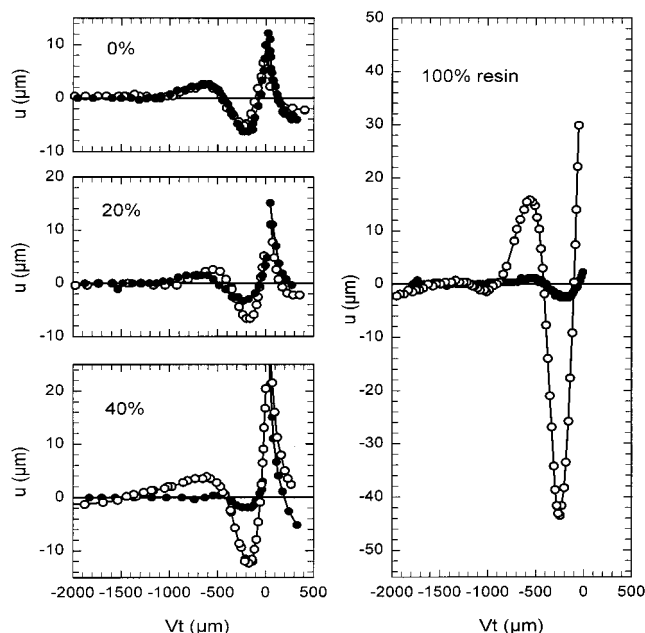


**Figure 6.** Displacements in the volume  $u_v$  (open symbols) and at the interface  $u_s$  (solid symbols) for elastomer substrates with resin contents 0%, 20%, and 40% (as indicated in the upper left corner) and on the pure resin layer (100%). The same scales are used for all the curves. Notice that, in the case of the pure resin layer, the peel front presented such a pronounced finger pattern that it was not possible to follow the displacement of the tracking particle.

40% MQ resin and the substrate made from 100% resin in Figure 6.

It is apparent that  $u_v$  increases gradually with the resin content, reaching large values. On the pure resin layer, the amplitude of the movement reaches  $\sim 100 \mu\text{m}$ , which is 3 times the initial thickness of the adhesive. For the pure PDMS elastomer,  $u_s$  and  $u_v$  appear superimposed, implying a negligible shear deformation inside the adhesive. For 40% or 100% resin, the difference between  $u_v$  and  $u_s$  is large, indicating a strong shear deformation within the adhesive. It can thus be expected that, for the samples with high resin content, an important part of the peel energy corresponds to energy dissipated within the sheared adhesive layer.

On the other hand, for elastomers without resin, slip motions at the adhesive/elastomer interface are extensive. Energy dissipation due to interfacial friction is then expected to be important.

One has to notice that in the case of the pure resin substrate, a small displacement at the interface is detected. Due to the high displacement gradient and to the finite size of the tracking particle (1  $\mu\text{m}$ ), the measured  $u_s$  represents an average displacement over the size of the tracking particle and not really a surface displacement. Assuming the true interfacial displacement to be zero, and a linear displacement profile, the corresponding displacement amplitude 1  $\mu\text{m}$  over the interface is on the order of  $u_v/a \sim 5 \mu\text{m}$  ( $a \sim 17 \mu\text{m}$  is the half-thickness of the adhesive), which is indeed the measured displacement.

**Kinetic Effects.** Peel tests were also performed after shorter contact times  $t_c$  between the adhesive and the silicone substrate. Peel curves all shift toward higher  $G$  values when the contact time increases. More interestingly, qualitatively different  $G$ – $V$  dependencies were obtained depending on the resin content. Figure 7 compares  $G$  versus  $V$  curves at three different contact times for elastomers with 0% and 40% MQ resin. For the



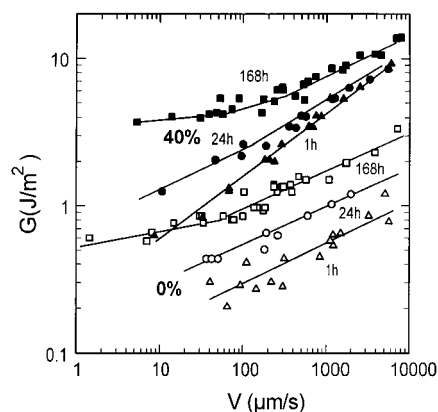


**Figure 7.** Comparison of the kinetics of adhesion enhancement for an elastomer containing 40% resin and a pure PDMS elastomer. Note that the slope of the  $G(V)$  curve for the pure elastomer does not change with contact time (slope  $\sim 0.3$ ), whereas there is a qualitative change of the shape of curve  $G(V)$  with increased contact time for the elastomer with 40% resin.

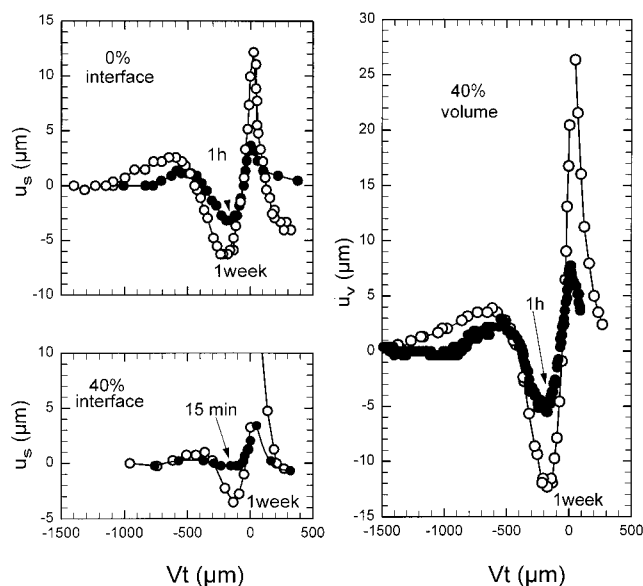


**Figure 8.** Evolution of the displacement with contact time. These figures compare the displacement  $u$  after a short or long time of contact prior to peeling. The contact time, the localization of the probe, and the nature of the elastomer are indicated for each curve.

0% elastomer, the  $G-V$  curves remain parallel on a double logarithmic plot. For the 40% resin content elastomer, the slopes of the  $G-V$  curves on a double logarithmic plot decrease as  $t_c$  is increased.

The displacements  $u_s$  and  $u_v$  corresponding to short contact times were also monitored. The amplitude of both displacements are smaller at short contact times (15 min) compared to long ones (1 week) as shown in Figure 8. Again, we checked that the trajectories plotted versus  $Vt$  were independent of the peel velocity. It seems therefore that the displacements depend only on the contact time between the adhesive and the elastomer prior to peeling.

### Discussion

The amount of MQ resin in the elastomer is likely to affect both the bulk viscoelasticity and the interactions with the acrylic adhesive. We have seen that it also affects the amount of interfacial slip and that a rupture with high slip was associated with small peel energy. The

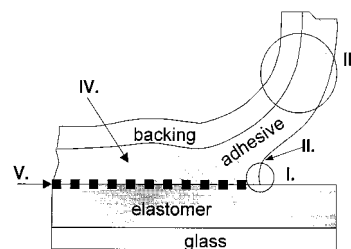


**Figure 9.** Sketch of the different zones involved in the dissipation of the peel work. I, dewetting line; II, elongational deformation; III, zone of large rotation; IV, volume behind the delamination front; V, zone of possible slip.

question is to know whether the control of interfacial slip is an efficient mechanism for varying the level of peel force.

The different zones responsible for dissipation of the peel energy are schematically presented in Figure 9. The mechanisms in zones I and V are directly linked to the interface, whereas for zones II–IV, dissipation occurs in bulk. In the classical picture of adhesion of viscoelastic bodies,<sup>9,10</sup> the adhesive energy  $G$  is the product of the adhesion energy  $W$  (zone I), often estimated on the basis of wetting measurements, and a dissipation function  $\Phi(V)$ , which accounts for the bulk viscoelastic dissipation in zones II–IV. In the case of two viscoelastic adherends, both sides of the assembly should contribute to  $\Phi$  (zones similar to II and III exist in the elastomer too).

The MQ resin affects both the surface and bulk properties of the elastomer. Can the modification of the bulk dissipative character of the elastomer explain the evolution of the peel force with resin content, as proposed by Gordon et al.<sup>11</sup> We first address this question.

The results presented above show large differences for the displacements, both at the interface and in the bulk, depending on the resin content. The shape of the displacement curves will be discussed first. Then, using additional data, we shall show that it is possible to estimate the dissipated energies associated with the movements at the interface and within the bulk of the adhesive. Finally, the possible interaction mechanisms allowing the interface between the elastomer and the adhesive to sustain a shear stress will be discussed.

**Relative Influences of the Surface Energy and of the Bulk Rheology of the Silicone Elastomer.** As the surface energies of the elastomers do not depend much on the resin content, the work of adhesion  $W$  for the adhesive–elastomer system should also be nearly independent of the resin content. Indeed, the value of  $W$  has been measured by the Johnson, Kendall, Roberts (JKR) method for the same elastomers but on a different acrylic adhesive.<sup>12</sup> A slight increase was observed, from  $46 \pm 4$  mJ/m<sup>2</sup> up to  $54 \pm 4$  mJ/m<sup>2</sup> when going from 0% to 40% in resin content into the elastomer. Thus the enhancement of peel energy with increasing resin content cannot be attributed to an increase in  $W$  associated with an increase in the polarity of the elastomer due to the resin.

On the contrary, we have seen that the mechanical properties of the elastomers are very sensitive to the resin

(9) Gent, A.; Schultz, J. *J. Adhes.* **1972**, *3*, 281–294.

(10) Andrews, E. H.; Kinloch, A. J. *Proc. R. Soc. London, A* **1973**, *332*, 385–399.

(11) Gordon, G. V.; Perz, S. V.; Tabler, R. L.; Stasser, J. L.; Owen, M. J.; Tonge, J. S. *Adhes. Age* **1998**, *35*–42.

(12) Amouroux, N. Ph.D. Thesis, University Paris VI, 1999. (b) Amouroux, N.; Léger, L. Proceedings of the 4th European Conference on Adhesion, Garmisch-Partenkirchen, Germany, 1998; pp 65–67. (c) Amouroux, N.; Léger, L. Proceedings of the Annual Meeting of the Adhesive Society, Savannah, GA, 1998; pp 232–234.

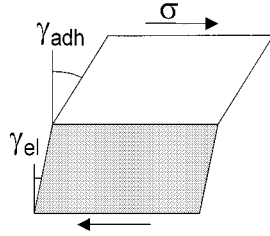


**Figure 10.** Sketch of a sandwich of elastomer and adhesive submitted to a sinusoidal displacement.

content. The loss modulus is 3 orders of magnitude larger for an elastomer with 40% resin than for a pure PDMS elastomer. It is then tempting to ascribe the enhancement in peel energy with resin content to the increase of the dissipative character of the elastomer.

However, under the effect of the peel force, both the adhesive and the elastomer are loaded. As the adhesive is much softer than the elastomers, it is expected to take the major part of the deformation. The net effect on the dissipation function may be estimated by considering the mechanical losses that would occur in a sandwich of adhesive and silicone elastomer submitted to an oscillating displacement. This situation is shown schematically in Figure 10. The ratio of shears in the elastomer and in the adhesive is given by

$$\frac{\gamma_{el}^*}{\gamma_{adh}^*} = \frac{\mu_{adh}^*}{\mu_{el}^*} \quad (1)$$

where the stars denote complex quantities. The ratio of the energies dissipated in one cycle per unit volume within the elastomer and the adhesive is

$$\phi = \frac{W_{el}^{diss}}{W_{adh}^{diss}} = \frac{\mu_{el}''}{\mu_{adh}''} \left| \frac{\gamma_{el}^*}{\gamma_{adh}^*} \right|^2 = \frac{\mu_{el}''}{\mu_{adh}''} \left| \frac{\mu_{adh}^*}{\mu_{el}^*} \right|^2 \quad (2)$$

Taking  $\mu' = 50$  kPa and  $\mu'' = 30$  kPa for the adhesive ( $\omega = 100$  rad/s), one obtains for the unfilled elastomer ( $\mu' = 250$  kPa and  $\mu'' = 1.7$  kPa) a ratio  $\phi \sim 2 \times 10^{-3}$  and for a 40% filled elastomer ( $\mu' = 3000$  kPa and  $\mu'' = 500$  kPa) a ratio  $\phi \sim 5 \times 10^{-3}$ . Furthermore, in real applications the thickness of the elastomer is typically 10 times smaller than that of the adhesive, which further reduces this ratio. Therefore, the major part of the viscoelastic dissipation takes place within the adhesive. In these systems, the tremendous increase of the dissipative character of the elastomer due to the resin is not the leading cause of the peel energy enhancement. Thus the conclusions of Gordon et al.,<sup>11</sup> based on a Gent and Schultz analysis,<sup>9</sup> are not able to explain the results presented here.

Before analyzing the processes in zones IV and V, we summarize the causes of the complex displacement field.

**Shape of the Displacement Curves.** Kaelble<sup>5,6</sup> modeled the peel test as a beam on an elastic foundation. The cleavage stress in the unpeeled zone was shown to be a sinusoidal damped function as a function of the distance  $x$  from the peel front, which is for a 90° peel geometry

$$\sigma = \sigma_0 e^{-\beta x} (\cos \beta x - \sin \beta x) \quad (3)$$

The maximum stress occurs at a distance  $1/2\pi\beta^{-1}$ , which depends both on the properties of the adhesive layer (thickness  $2a = 35$   $\mu\text{m}$ , Young modulus  $Y \sim 3\mu' \sim 0.067$

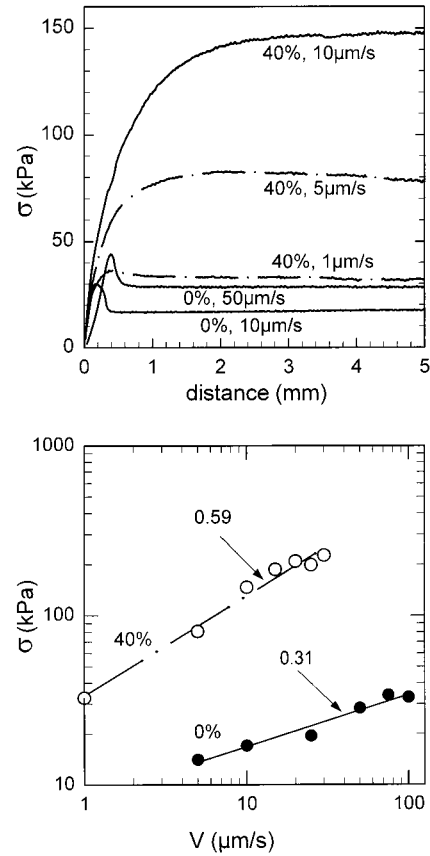


**Figure 11.** Estimation of the friction stress of the adhesive on elastomers 0% or 40% from a simple lap shear experiment. The plateau values are reported as a function of the sliding velocity and are found to follow power laws in the range investigated (lower panel).

MPa) and on the properties of the flexible backing (thickness  $h = 40$   $\mu\text{m}$ , Young modulus  $E \sim 1400$  MPa):

$$\frac{\pi}{2}\beta^{-1} = \frac{\pi}{2} \left( \frac{2ah^3E}{3Y} \right)^{1/4} \quad (4)$$

Inserting the materials' properties given above, this length is of order 550  $\mu\text{m}$  (460  $\mu\text{m}$  in the case of thickness 17  $\mu\text{m}$ ). This is very close to the position  $x_0 \sim 475$   $\mu\text{m}$  for which  $u$  is zero in all the probe trajectories presented in Figure 5 or Figure 6. This agreement confirms the coupling between the cleavage stress and the oscillatory lateral motion. Note that both the theoretical position given by expression (4) and the experimental  $x_0$  are independent of  $G$  or  $V$ . Close to the peel front the displacement changes sign again because of the Poisson contraction resulting from the vertical stretch of the adhesive in this zone. Kaelble<sup>5,6</sup> did observe this oscillatory lateral stress using a bi-axial bond stress analyzer (BBSA unit), even if not predicted by his simple elastic foundation model.

#### Evaluation of the Energy Dissipated by Friction.

The stress corresponding to a slip motion of the adhesive on the elastomer may be evaluated by measuring it directly in a pure shear single-overlap geometry. In such an experiment, the shear stress reaches a steady-state value, which depends on the velocity and on the elastomer substrate (see Figure 11). The steady-state values of the shear stress, measured after a short time of contact ( $\sim 15$  min), follow a power law:

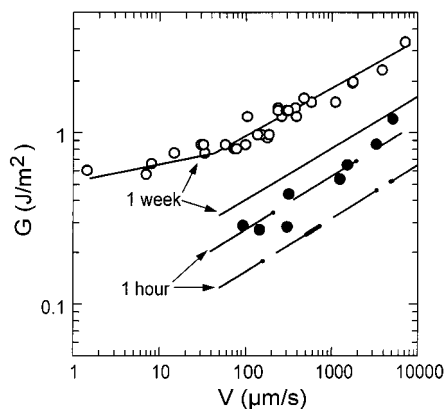


**Figure 12.** Comparison between the friction energy,  $G_f$ , and the peel energy,  $G$ , for the 0% elastomer after short and long contact times.

$\sigma_f(v) = (8300 \pm 1000)v^{0.31 \pm 0.03}$  for a pure silicone elastomer and

$\sigma_f(v) = (33\,600 \pm 3400)v^{0.59 \pm 0.04}$  for the 40% resin content elastomer.

The part of the peel energy due to interfacial slip may then be estimated by integrating the corresponding work over the whole contact area.<sup>7,8</sup> With a power law relationship for the frictional stress versus velocity, the energy dissipated by friction at a peel speed  $V$  is simply proportional to the stress evaluated at  $V$ :

$$G_f = \int \sigma_f v dt = \frac{1}{V} \int \sigma_f v dx = \left( \int \left| \frac{du}{dx} \right|^{\alpha+1} dx \right) \sigma_f(V)$$

where  $\alpha$  is the exponent of the power law relative to the dissipation function and  $v = du/dt = V du/dx$  is the local velocity of the adhesive near the interfacial plane, evaluated with the fluorescent probes.

This energy is about half of the peel energy measured at short or long contact times for a pure PDMS elastomer, as shown in Figure 12. Note the parallelism in double logarithmic plot between the curve  $G_{\text{friction}}$  and the peel curve. This is consistent with the results obtained by Newby and Chaudhury<sup>7,8</sup> on a thin layer of PDMS chains with a similar adhesive.

For a 40% resin content elastomer, peeled after a short contact time with the adhesive, the amplitude of the interfacial displacement is small, but since the friction stress is high, a large part of the peel energy is dissipated by friction. Again, the curves obtained from the friction law and the peel curve (Figure 13) are parallel. The friction energy is about 25% of the peel energy. For long contact times, the peel curve appears qualitatively very different, which means that another process takes place.

#### Evaluation of the Energy Dissipated in the Bulk.

The shear field in the adhesive may be estimated by the difference between the measured displacements in the midlayer  $u_v$  and the displacements in the vicinity of the interface  $u_s$ , divided by half the thickness of the adhesive. More accurately the displacement profile within the adhesive can be modeled by two straight lines of slope  $-u_v/a$  for  $a < z < 2a$  and  $(u_v - u_s)/a$  for  $0 < z < a$  ( $z = 0$  is the equation of the elastomer/adhesive interface). The corresponding stress is obtained from the estimated shear  $\gamma$  and the time dependent shear modulus  $\mu(t)$  by a convolution product:

$$\sigma(t, z) = \int_{-\infty}^t \mu(t - \tau) \frac{\partial \gamma}{\partial \tau}(t, z) d\tau \quad (5)$$

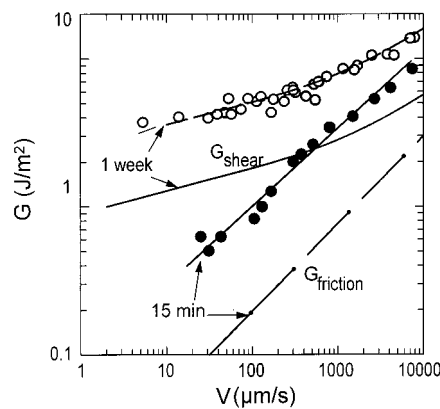


**Figure 13.** Comparison between the friction energy,  $G_f$  (---), and the peel energy,  $G$  (b), for the 40% elastomer at short contact time, and comparison between the energy dissipated by shear in the volume of the adhesive,  $G_{\text{shear}}$  (—), and the peel energy,  $G$  (O), for the same elastomer after a long contact time.

This equation may be written as a function of distance from the peel front by use of the equivalence  $x \leftrightarrow Vt$ :

$$\sigma(x, z) = \int_{-\infty}^t \mu\left(\frac{x - \xi}{V}\right) \frac{\partial \gamma}{\partial \xi}(\xi, z) d\xi \quad (6)$$

The energy dissipated in the bulk is given by

$$G_{\text{shear}} = \int \sigma \frac{\partial \gamma}{\partial x} dx dz \quad (7)$$

The time-dependent modulus of the adhesive may be approximated from the elastic dynamic modulus:<sup>13</sup>

$$\mu(t) \sim \mu'(1/\omega) \quad (8)$$

For a peel experiment on a 40% resin content elastomer,  $G_{\text{shear}}$ , estimated from the measured  $u_s$ ,  $u_v$ , and  $\mu'(\omega)$  by use of eqs 6–8, is about one-third of the peel energy measured at long contact times, as shown in Figure 13. The curve  $G_{\text{shear}}$  versus  $V$  is parallel to the peel curve over nearly four orders of magnitude of peel velocities, which further confirms the bulk viscoelastic origin of the dissipated energy.

Others sources of dissipation localized in zones I–III should account for the difference between  $G_{\text{shear}}$  and  $G$ . Note that  $G_{\text{shear}}$  does not include losses due to the stretching of the adhesive perpendicular to the interface. This stretching energy could be of the same order of magnitude as  $G_{\text{shear}}$  since stretching and shear are coupled in this zone.

**Interfacial Interactions.** In all cases, we have observed that the peel energy depends strongly on contact time. In the case of a pure PDMS elastomer, this enhancement may be explained by molecular effects such as dipole–dipole orientation, which should increase  $W$ , or mechanical effects such as relaxation of residual stresses. Whatever the contact time, however, the interactions between the PDMS elastomer and the adhesive remain so weak that the interface is not able to resist shear and the peel proceeds through interfacial slip.

The building of the interface in the case of an elastomer rich in resin should be different. When exposed to air, the elastomer surface is plausibly richer in PDMS than in resin, due to the weaker surface tension of the former.

(13) See, for example, Ferry, J. D. *Viscoelastic Properties of Polymers*, Wiley and Son: NY, 3rd ed.; 1980; p 69.



This situation should evolve when the elastomer is brought into contact with the adhesive. The segmentally mobile PDMS chains should then move slightly to let the resin particles emerge and finally interact with the adhesive. This mechanism could explain the transition from a rupture mechanism associated with slip and interfacial friction at short contact times, to a blocked interface and bulk viscoelastic dissipation at long contact times. The increase of interfacial interactions with time was also observed by JKR experiments.<sup>12</sup>

It is now well-known that the hydrodynamic rule of no slippage for a fluid flowing over a substrate does not hold for polymers. For an entangled melt, slip is favored since a zero velocity condition would require disentanglement close to the interface.<sup>14</sup> Slip effects were experimentally first directly demonstrated by Migler et al.<sup>15</sup> Recently it has been shown by Pit et al.<sup>16</sup> that even a simple fluid such as hexadecane could slip on a solid substrate, depending on its surface preparation. From model experiments involving polymer melt flowing over a surface able to adsorb chains, we know that slip is highly reduced at low shear rates due to entanglements between the surface-anchored chains and the melt. If the surface is protected by a thick and dense layer of grafted chains, the interaction with the melt is reduced and large slip is observed.<sup>17</sup> In the case of immiscible polymers, slip is favored since the interactions are weak. Recent experiments, in simple shear flow geometry, indeed showed that a styrene-butadiene (SBR) melt experienced huge slip (plug flow) on a PDMS brush.<sup>18</sup>

The interface between the adhesive and the elastomer without resin is very similar to that between immiscible polymers. The interface should not be able to sustain shear. Under shear, slip is extensive. As peel implies shear, the peel front is associated with slip and the dissipation is dominated by friction at the interface. Increasing the resin content in the elastomer tends to decrease interfacial slip motions. Even if the exact nature of the interactions between the polymer chains in the adhesive and the resin particles is still under question, we think that the resin particles are likely to play the role of anchoring sites for the acrylic chains of the adhesive, preventing large slippage, in a way somewhat similar to what entangled grafted chains do. The high peel energy observed for the substrate of pure resin is indeed an indication of a strong interaction, along with the observation that when the adhesive was left in contact with the resin layer for a long time (months), there was a dissolution of the resin layer in the adhesive. If the interface is able to sustain shear stress, the adhesive becomes highly deformed, and the peel energy is dominated by dissipation through shear in the adhesive layer.

The nonlinear evolution of  $G$  with the resin content is thus linked to a transition from surface to bulk dissipation. This change in dissipation mechanisms is related to the interfacial resistance to shear stress.

### Conclusion

We have demonstrated that, for a silicone elastomer versus an acrylic soft adhesive, an important factor affecting peel strength was the possibility of slip motions at the interface. For small silicone MQ resin contents in

the PDMS matrix, interfacial slip is extensive and the peel energy is low, whereas for large amount of resin, slip is limited and shear develops in the bulk of the adhesive, giving viscoelastic dissipation. The bulk loss properties of the silicone elastomers are believed to be unimportant for this process. The peel force is enhanced when the dissipative character of the adhesive is excited. The surface properties of the elastomer, or more accurately its ability to interact with adhesive chains to form surface-anchored chains able to sustain shear stresses are the key point. The control of slip at the interface thus appears as an efficient way to adjust the peel force.

### Experimental Section

**Silicone Substrates.** Silicone elastomers were prepared from poly(dimethylsiloxane) (PDMS) and MQ silicone resin in various proportions. The divinyl-terminated poly(dimethylsiloxane) ( $M_n = 17\,000$  g/mol by titration,  $I = M_w/M_n = 1.3$  by GPC) was obtained after several precipitations in acetone of a commercial-grade silicone oil (Rhodia 621V200). The silicone MD<sup>VI</sup>Q resin (Rhodia) was used as received. The chemical composition was estimated by <sup>29</sup>Si NMR ( $M = \text{Me}_3\text{SiO}_{1/2}$ , 47.3 wt %;  $\text{D}^{\text{VI}} = \text{ViMeSiO}_{2/2}$ , 9.1 wt %;  $\text{Q} = \text{SiO}_{4/2}$ , 43.6 wt %). The ratio O/Me is close to unity and thus the resin is expected to be less apolar than PDMS, which has two methyl groups for one oxygen. From small-angle X-ray scattering experiments we know that the resin particles are compact structures with gyration radii  $R_g = 1\text{--}2$  nm. The corresponding average molecular mass is in the range 3000–5000 g/mol. Blends of PDMS and resin (0 wt % up to 40 wt % in resin) were prepared and the concentration of vinyl groups was titrated.<sup>19</sup> The catalyst (Karstedt's Pt) is added at a concentration of 20 ppm Pt for  $10^{-4}$  mol of vinyl groups. After addition of 1,3,5,7-tetramethyltetracyclosiloxane ( $\text{D}^4$ ) which acts as a four functional cross-linker, the mixture is stirred for 15 min, degassed and then deposited on glass slides. In the case of the mixture without MD<sup>VI</sup>Q, the potlife at ambient temperature is short; therefore the stirring of the  $\text{D}^4$  was done at  $-15^\circ\text{C}$  under a dry nitrogen atmosphere. To ensure a good anchoring of the silicone elastomer, the glass slides were previously etched with Piranha [1:1  $\text{H}_2\text{SO}_4$  (98%): $\text{H}_2\text{O}_2$  (50%)]. The samples were cured overnight at  $100^\circ\text{C}$ . The relative quantity of  $\text{D}^4$  was adjusted so as to minimize the sol fraction ( $r = [\text{SiH}]/[\text{C}=\text{C}] = 1.2$  for pure PDMS and  $r = 1.7, 1.8, 1.95$ , and  $2.2$  for 10, 20, 30, and 40 wt % resin, respectively). The thickness of the elastomer layers on glass is  $60\ \mu\text{m}$ . Mechanical dynamic properties were probed with a Rheometrics RSAII solid analyzer at  $25^\circ\text{C}$  using elastomer prepared in the same way but made thicker (1 mm). Surface energies were characterized by dynamic tensiometry with  $\text{H}_2\text{O}$  and tricresyl phosphate. The pure resin layer was made by spin-coating on a glass slide a solution containing 5% resin in toluene.

**Adhesive.** A supported acrylic adhesive tape, Scotch 3M 600, was used. The dynamic mechanical properties were characterized with a Rheometrics RMS 800 liquid analyzer. Sandwiches of 10 tape layers were placed between the parallel plates of the rheometer. The backing made of cellulose acetate is supposed not to interfere because of its high Young modulus ( $E = 1.4$  GPa). Complex shear modulus was measured for frequencies between  $10^{-1}$  and  $10^2$  rad/s at different temperatures ranging from  $-30$  to  $50^\circ\text{C}$ . The time temperature superposition principle was applied to obtain a master curve at a reference temperature of  $T_0 = 25^\circ\text{C}$  shown in Figure 2. Horizontal  $a_T$  shift factors were in accordance with the WLF equation taking  $C_1 = 9.6 \pm 0.6$  and  $C_2 = 190 \pm 13^\circ\text{C}$ . No vertical shift factors were used.

**Fluorescent Probes.** Fluorescent latex probes (Molecular Probes 505/515) were placed either at the surface of the adhesive tape or in the midlayer of doubled tapes. Dilute (10–20 ppm) latex solution in water was prepared and a thin film of the solution was applied directly on the adhesive surface. The adhesive tape

(14) De Gennes, P. G. *C. R. Acad. Sci. Paris* **1979**, *288*, 219–220.

(15) Migler, K. B.; Hervet, H.; Léger, L. *Phys. Rev. Lett.* **1993**, *70*, 287–290.

(16) Pit, R.; Hervet, H.; Léger, L. *Phys. Rev. Lett.* **2000**, *85*, 980–983.

(17) Durlat, E.; Hervet, H.; Léger, L. *Eur. Phys. Lett.* **1997**, *38*, 383–388.

(18) Léger, L.; Hervet, H.; Charitat, T.; Koutsos, V. *Adv. Colloid Interface Sci.* **2001** (in press).

(19) The silicone is diluted in  $\text{CCl}_4$  and a given excess quantity of IBR is added in the presence of mercuric acetate as catalyst. After 15 min, an aqueous solution of KI in excess is added. The iodine resulting from the reaction of KI on unreacted IBR is then titrated with sodium hyposulfite. The quantity of vinyl groups is then straightforwardly inferred from this measurement.

was then immediately dried in an oven (40 °C). Doubled tapes were obtained by the protocol of Newby and Chaudhury.<sup>7,8</sup> The tape is first stuck on the bottom of a polystyrene Petri dish, which is then filled with water. After a few hours the backing film (cellulose acetate) can be removed easily and the adhesive is dried. An adhesive tape sparingly coated with probes is then applied on the unbacked adhesive film. The doubled tape is removed by a fast peeling action. The diameter of the probes used is 1  $\mu\text{m}$  for latex on surface and 2  $\mu\text{m}$  for latex placed in the midlayer. The thickness of the doubled adhesive film is 35  $\mu\text{m}$ . The thickness of the backing is 40  $\mu\text{m}$ .

**Peel Test.** Peel tests were conducted under microscope with dead weights. The mechanical energy release rate for this 90° peel test is simply given by

$$G = \frac{mg}{b} \quad (9)$$

$mg$  being the dead weight ( $m$ , mass;  $g$ , acceleration of gravity) and  $b$  the width of the peeling strip (19 mm). The Polyvar microscope working in reflection is equipped with an epifluorescent accessory (Omega filters), which allows visualization of the fluorescent latex probes. A 50 $\times$  objective is used. The movement of the probes and the peel front are monitored with a sensitive camera (LHESA) and recorded on videotape. The trajectory of the probe is reconstructed thanks to a specific program that picks a chosen line (crossing the peel front and passing through the probe) from video images corresponding to fixed intervals of time and builds a spatiotemporal image out of these lines. Typically 30 points of the spatiotemporal image are taken from the trajectory to allow for an easier comparison between curves. The accuracy of the measurement of the position of the probe is about 1  $\mu\text{m}$ . The peel velocity  $V$  is deduced from the slope of the trajectory corresponding to the peel front.

Peel tests were also conducted outside the microscope, at imposed force by use of dead weights or at imposed velocity by use of an Instron tensile machine in the case of the substrate with pure resin.

### Nomenclature

$a$  = thickness of the adhesive (half thickness in the case of doubled tape)

$\alpha$  = exponent of the power law describing the friction stress as a function of slip velocity

$b$  = width of the adhesive tape

$\beta^{-1}$  = theoretical wavelength of the oscillatory stress

$E'$  = elastic component of the complex Young modulus of the elastomer

$E''$  = loss component of the complex Young modulus of the elastomer

$\phi$  = estimated ratio of energies dissipated in the bulk of the elastomer and in the adhesive

$\Phi$  = dissipation function

$G$  = mechanical energy release rate

$G_{\text{friction}}$  = energy dissipated by interfacial friction

$G_{\text{shear}}$  = energy dissipated by shear deformation in the adhesive

$\gamma$  =  $du/dz$  = shear in the adhesive

$\gamma_i, \gamma_{ij}$  = surface or interfacial energy

$h$  = thickness of the backing

$\mu'$  = elastic component of the complex shear modulus of the adhesive

$\mu''$  = loss component of the complex shear modulus of the adhesive

$\sigma$  = shear stress

$\sigma_f$  = friction stress

$t$  = time

$t_c$  = time of contact prior peeling

$u_s$  = interfacial displacement

$u_v$  = displacement in the bulk (midlayer)

$v = du/dt$  = speed of displacement

$V$  = peel velocity

$W$  = Dupré work of adhesion

$\omega$  = pulsation in dynamic mechanical analysis

**Acknowledgment.** We are indebted to Rhodia Silicone for financial support and for providing us the MQ resins.

LA010146R